Available online at www.sciencedirect.com

ScienceDirect

Ceramics International 41 (2015) 10406–10414

CERAMICS INTERNATIONAL

www.elsevier.com/locate/ceramint

Simple and cost-effective method to obtain RE^{3+}-doped Al_2O_3 for possible photonic applications

Daiane H.S. Reis[a], Juliana M.M. Buarque[a], Marco A. Schiavon[a], Edison Pecoraro[b], Sidney José L. Ribeiro[b], Jefferson L. Ferrari[a,*]

[a]*Grupo de Pesquisa em Química de Materiais – (GPQM), Departamento de Ciências Naturais, Universidade Federal de São João del-Rei, Campus Dom Bosco, Praça Dom Helvécio, 74, 36301-160 São João Del Rei, MG, Brazil*

[b]*Instituto de Química, UNESP, P.O. Box 355, 14800-970 Araraquara, SP, Brazil*

Received 30 March 2015; received in revised form 15 April 2015; accepted 16 April 2015
Available online 25 April 2015

Abstract

Materials containing rare earth ions with photoluminescent properties have been investigated as efficient phosphors for applications in photonics. In this work We reports on preparation of Eu^{3+}-doped Al_2O_3 with different concentrations of Eu^{3+}, in relation to the amount of moles of Al^{3+}, has been prepared using a simple and inexpensive synthesis. XRD showed that the alumina-based materials calcined at 400 and 600 °C were predominated by the γ-Al_2O_3 phase. However the materials heat-treated above 800 °C showed mixture of γ and α-Al_2O_3 phases. SEM presented results demonstrating that the heat-treatment at increased temperature favors a larger particle size with inhomogeneous morphology. It was observed with photoluminescence spectroscopy that theEu^{3+}-doped Al_2O_3 materials showed intense photoluminescence emission around 612 nm under excitation at 394 nm. This emission in the visible region was assigned to a down-shifting phenomenon attributed to the intraconfigurational f–f transitions of Eu^{3+}. Intense emission around 693 nm assigned to Cr^{3+} were observed, and the intensity is controlled by the heat-treatment temperature of synthesis. The lifetime found for these materials are of the order of milliseconds at 612 nm. In summary the materials obtained in this work show properties than can be used for photonics applications.

Keywords: Aluminum oxide; Rare earths; Photoluminescence; Oxides

1. Introduction

In recent years, the development of new technologies has inspired a great interest in developing new materials for applications in photonics and nanophotonics. Among the various kind of materials, those containing Rare Earths ions (RE^{3+}) have been investigated as efficient phosphors for application in high-tech systems [1–2]. They are usually very well-known materials because of its use in traditional lighting displays and devices such as cathode ray tubes, fluorescent lamps, LED, lasers [3], and field emission displays, among others. These materials should provide high quality image generation [4,5] and optical light [6]. In these examples, generally a source of ultraviolet (UV) radiation excites the materials which absorb energy and emit preferably in the visible region.

It is well known that RE^{3+} such as Eu^{3+}, Sm^{3+}, and Tb^{3+} exhibit a significant amount of luminescence in the visible light region. In recent years, studies on the development of luminescent materials using RE^{3+} have attracted much attention. These materials may transform the energy absorption in the shorter wavelength region to the energy of luminescence in the wavelength region with high luminosity [7]. The RE^{3+} have been chosen for study as doping because they are extremely useful in optical applications due to their crisp and monochromatic emission lines [8–9]. Through the electron spectroscopy (absorption and emission), the investigation of the chemical environment is possible, making these suitable as spectroscopic probe [10].

*Corresponding author. Tel./fax: +55 32 3379 2481.
E-mail addresses: ferrari@ufsj.edu.br, jeffersonferrari@gmail.com (J.L. Ferrari).

http://dx.doi.org/10.1016/j.ceramint.2015.04.086
0272-8842/

Among the different RE^{3+}, commonly used as dopants in a variety of different materials, europium ions (Eu^{3+}) have attracted great attention because of their photoluminescence properties when present in a host matrix, which gives potential use as emitting phosphors light, electroluminescent devices, optical amplifiers or lasers [11], high-density optical storage [12], and others.

The luminescence spectrum of Eu^{3+} has emission lines extending from the visible to near infrared. Emissions are coming from energy levels that generate state transitions assigned to the $^5D_0 \rightarrow {}^7F_J$ ($J=0$, 1, 2, 3, 4, .., 6). Their transitions, especially between states $^5D_0 \rightarrow {}^7F_2$ (known as hypersensitive transition) allows determining the site of symmetry of the ion [13–14]. Typically, in inorganic systems, the Eu^{3+} is excited at 394 nm (level $^5L_6$), decays to ^5D_J levels, especially for $^5D_0$, which causes an intense luminescence [9], depending on the enviromental..

The selection of host matrix is fundamental for the development of luminescent materials because a given luminescent center has different optical properties in different matrices [15]. A suitable host for RE^{3+} ions primarily provides a great energy of the forbidden zone, with good solubility and chemical stability [16–18].

The search for new photoluminescent materials, has led to investigations into the photoluminescence of RE^{3+} in aluminum oxide (Al_2O_3). This has been extensively studied as a host material for the RE^{3+} [7,19–22] because its thermal stability is increased upon doping with these ions [10,23]. Alumina (Al_2O_3) presents different crystalline structures. It is believed to have more than 15 different crystallographic phases, which can be subjected to a variety of transitions until the most stable structure, corundum (Al_2O_3) is obtained with an energy gap around E_g=9.4 eV [24,26–28]. Other alumina phases include γ, δ, η, θ, κ, β, χ which are metastable polymorphs. These are called transition phases, acting as intermediate phases in the steps preceding the α phase during heating-treatment [29]. Among the transition phases, the most popular is γ-Al_2O_3, due to its application as a catalyst [24]. Another consideration is the viability of obtaining materials with great photoluminescent properties with affordable manufacturing.

Within this context, this work is based primarily on the preparation of Eu^{3+}-doped Al_2O_3 with different percentages. Characterization of the structural properties is performed to assess the best photoluminescent properties of this material, through the methodology used for the synthesis.

2. Experimental procedure

Among the various techniques for synthesis of inorganic solid compounds, materials based on aluminum oxide (Al_2O_3) doped with different concentrations of the Eu^{3+} were prepared by a co-precipitation method. This technique enables greater homogeneity among the reactants contributing to the distribution of particle size. In addition, this route promotes the simplicity of the synthesis process and a low energy to start the reaction. The precursors used in this work were rings of aluminum cans and a rare earth oxide (Eu_2O_3 Estarm—99.99%), previously standardized with 0.01 mol L^{-1} EDTA. Initially 0.5 g of rings of aluminum can was dissolved in 13 ml of 5.0 mol L^{-1} HCl with stirring and heating at 60 °C for 15 min. After complete dissolution of the rings of aluminum cans, the doping was performed with 1, 2, 3 and 5 mol% of Eu^{3+} in relation to the total number of Al^{3+} moles. Then, 7 mL of ammonium hydroxide was added to precipitate aluminum hydroxide. The precipitate was centrifuged and kept in a oven at 100 °C for 4 days. The materials were crushed in an agate mortar to obtain

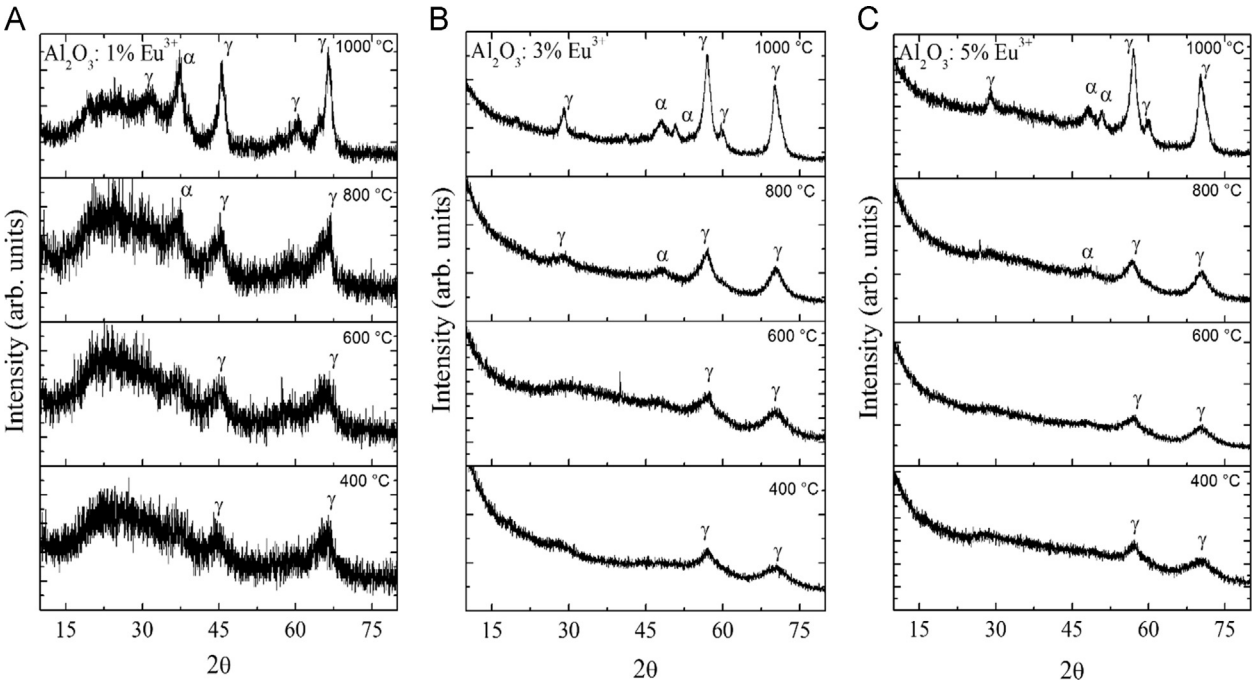

Fig. 1. XRD patterns of the Eu^{3+}-doped Al_2O_3 samples with: (A) 1, (B) 3, and (C) 5 mol%, heat-treated at 400, 600, 800 and 1000 °C for 4 h prepared by co-precipitation method.

powders which were heat treated at 400, 500, 600, 700, 800, 900 and 1000 °C for 4 h to obtain Eu^{3+}-doped Al_2O_3 photoluminescent materials.. The identification of the crystalline phases of the samples were performed by X-ray diffraction (XRD), operating the LabX difractometer-6000 (Shimadzu) with a Cu-Kα radiation ($\lambda = 1.5418$ Å), and a Cr-Kα radiation ($\lambda = 2.2910$ Å) with scan rate of 0.2°/min between $2\theta = 10$–80° and graphite monochromator. The morphology and surface analysis of the particles of the materials were evaluated by scanning electron microscopy SEM (Hitachi TM 3000). The energy dispersive x-ray spectroscopy (EDS) was used to quantify the composition of the system. The photoluminescence spectra were acquired at room temperature using a spectrofluorimeter SPEXF2121/Jobin-Yvon Fluorolog. The emission spectra were collected in the interval between 570 and 720 nm. Initially they were obtained the emission spectra with excitation at 394 nm. The excitation spectra were obtained in interval between 350 and 550 nm, fixing the emission at 612 nm. The slits used for obtaining the emission and excitation spectra were 2 and 3 nm for the excitation and emission monochromator, respectively. The filter used in the emission spectra was 399 nm cut-off. The lifetimes were collected fixing the emission and excitation at 612 and 394 nm, respectively.

3. Results and discussion

From the X-ray diffraction (XRD), the structural properties were determined, the crystalline network and the degree of crystallinity of the materials obtained. Fig. 1(A) shows the XRD patterns of the Eu^{3+}-doped samples with 1 mol% of Eu^{3+} using copper radiation, and the XRD patterns of the samples doped with 3 and 5 mol % of Eu^{3+} using chromium radiation are shown in Fig. 1(B) and (C), respectively. The peaks observed in the X-ray pattern in Fig. 1 (B) and (C) were obtained using the Cr-Kα, can be considered and compared to the same peaks obtained in the X-ray diffraction in Fig. 1(A) using the Cu-Kα. In comparison to the cooper radiation, the wavelength of the chromium radiation provoke a shift of the peaks to the higher values of theta, in accordance to the Bragg's Law, and the results can be observed in Fig. 1.

According to the results obtained by XRD, the samples heat-treated at 400–600 °C, independent of the concentration of RE^{3+}

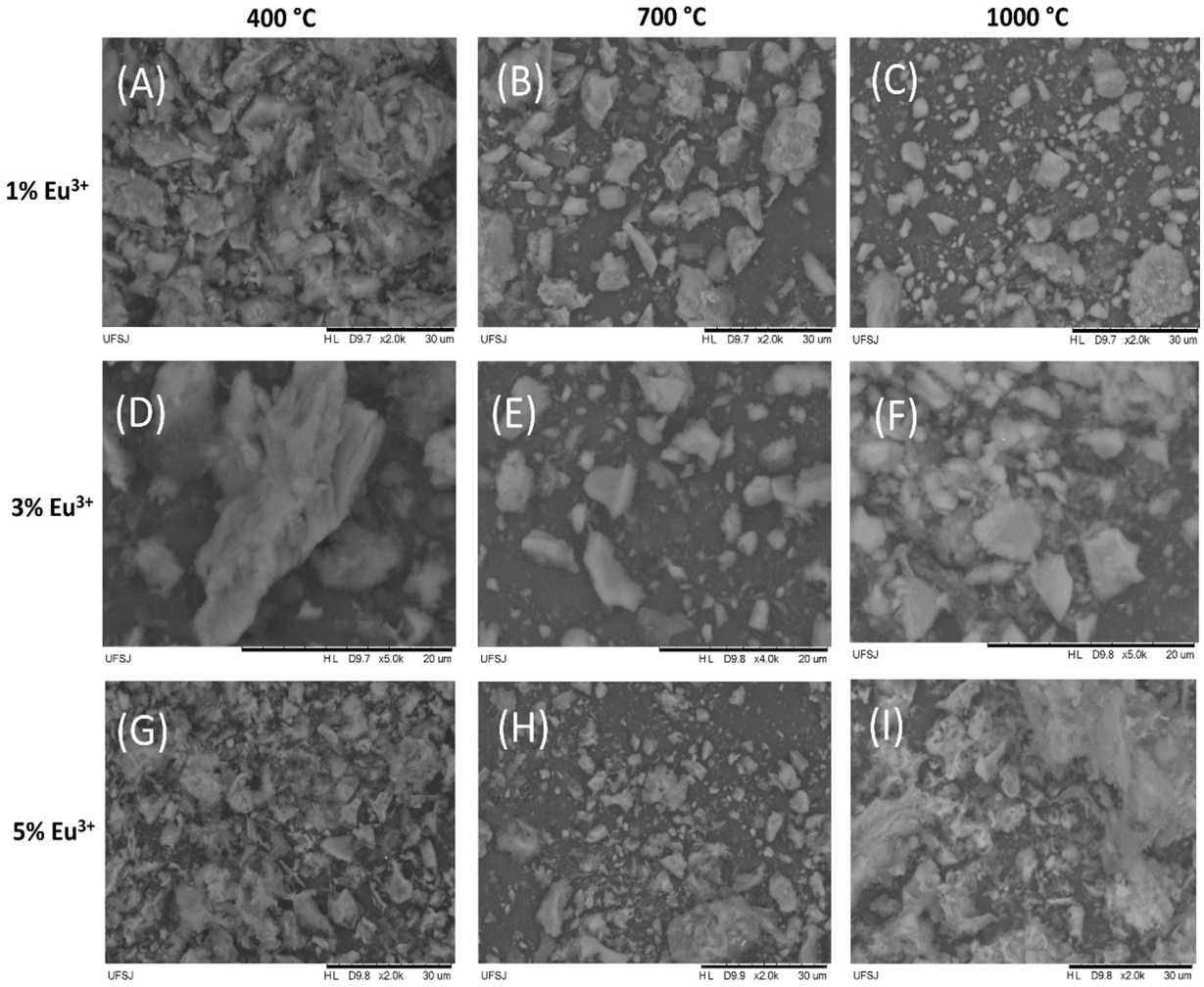

Fig. 2. SEM images of the Eu^{3+}-doped Al_2O_3 withdifferent percentages, heat-treated at different temperatures for 4 h prepared by co-precipitation method: (A), (B), (C) 1mol% heat-treated at 400, 700, 1000 °C, respectively, (D), (E), (F) 3 mol% heat-treated at 400, 700 and 1000 °C, respectively, and (G), (H), (I) 5 mol% heat-treated at 400.700 and 1000 °C, respectively.

in the matrix, showed broad peaks with most intense reflection positioned at $2\theta = 45.6^\circ$ and 66.6° assigned to the (400) and (440) *hkl* plane, respectively. These peaks are attributed the cubic phase (γ-Al_2O_3) according to the crystallographic card JCPSDS 00-050-0741. Increasing the heat-treatment temperature, the formation of large peaks characteristic of a crystalline structure attributed to the stable corundum hexagonal phase of alumina (α-Al_2O_3) with the cubic phase is observed. . The transition from γ-Al_2O_3 phase to the hexagonal phase α-Al_2O_3, is due to transition from intermediate phases present in the process of obtaining the α-Al_2O_3 phase during the heat-treatment of the sample. Therefore, samples heat-treated at 800–1000 °C presented a system with a mixture of the two phases–γ-Al_2O_3 and α-Al_2O_3.

Scanning electron microscopy (SEM) was used to obtain information on the morphological characteristics of the Eu^{3+}-doped alumina powders with 1, 3 and 5 mol%, and heat-treated at different temperatures. Fig. 2 shows micrographs obtained. The micrographs show different shapes and particle sizes. An increase of heat-treatment temperature favors the formation of agglomerates and larger heterogeneous morphology, which are associated with sintering during the heat-treatment process. It is believed that the narrow peaks observed in the XRD of the samples treated at 1000 °C, are associated with the presence of larger particles dispersed in the crystal lattice of α-alumina. The micrographs shown in Fig. 3, demonstrate the behavior of the Eu^{3+}-doped Al_2O_3 with different concentrations heat-treated at the same temperature. It is observed in micrographs of matrices doped with higher concentrations of Eu^{3+}, the particles formed have clusters with larger sizes compared to the others. In general, the samples containing different percentages of Eu^{3+} heat-treated at the same temperature exhibit heterogeneous morphology of the particles.

The samples were also analyzed by energy dispersive X-rays and the quantitative results obtained are shown in Fig. 4. The results presented are representative for the samples obtained in this work. The histograms are related to the quantity of each element present in the obtained alumina sample.

It can be seen in Fig. 4 that both have an atomic percentage of 1–2.9% of Eu^{3+}. These values are consistent with the concentration of dopant incorporated in the Al_2O_3 matrix, which were 1 and 3 mol% during the synthesis. Fig. 5 shows the results of EDX for the rings of aluminum cans used as Al^{3+} precursors. The rings of aluminum cans used have a relatively low percentage of Cr metal. The presence of Cr in the composition of the ring of aluminum cans is attributed to chromium plating process used in industry to prevent the oxidation of this material.

In order to analyze the photoluminescent properties of the obtained materials, the materials formed were submitted to the analysis of photoluminescence spectroscopy. Initially alumina samples doped with 1 mol% of Eu^{3+} heat-treated at different

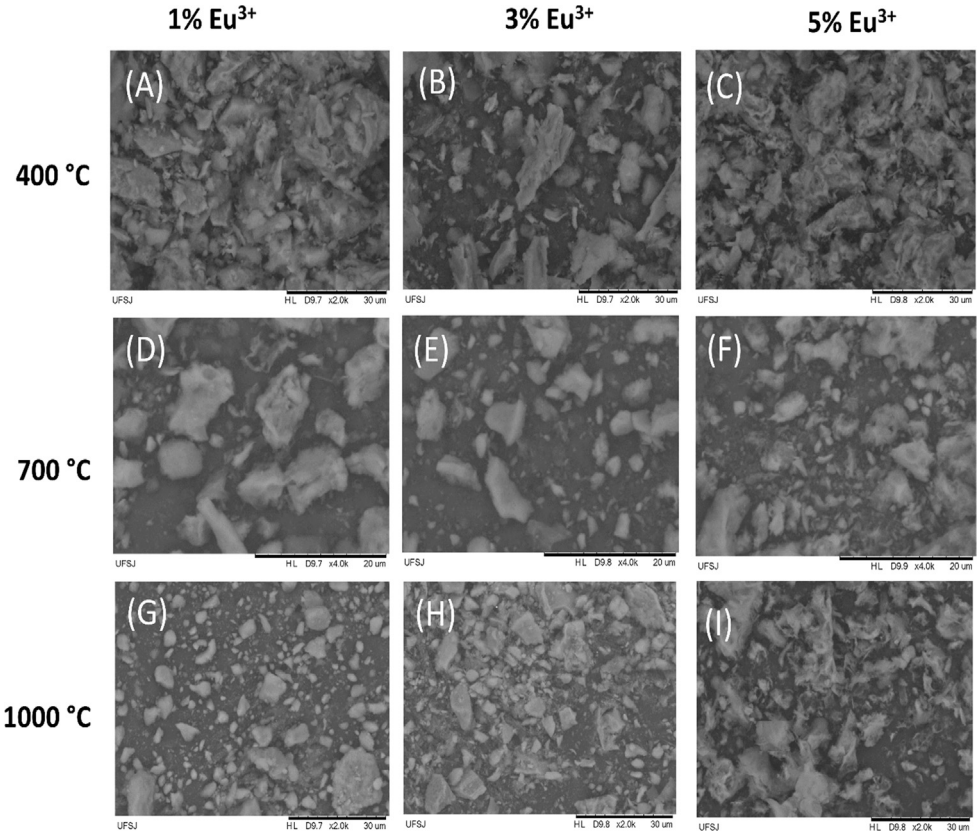

Fig. 3. SEM images of the Eu^{3+}-doped Al_2O_3 with diferents percentages heat-treated at different temperatures for 4 h prepared by co-precipitation method: (A), (D), (G) 1 mol% heat-treated at 400, 700, 1000 °C, respectively, (B), (E), (H) 3 mol% heat-treated at 400, 700 and 1000 °C, respectively, and (C), (F), (I) 5 mol% heat-treated at 400, 700 and 1000 °C, respectively.

temperatures were submitted to photoluminescent excitation analysis. Thus, it was found the best wavelength to excite the materials. Fig. 6 shows the excitation spectra of the samples Eu^{3+}-doped Al_2O_3 1 mol% heat-treated at different temperatures. These spectra were recorded between 350 and 550 nm, and wavelength of emission fixed in the hypersensitive transition, $^5D_0 \rightarrow {}^7F_2$, in 612 nm.

Shown in Fig. 6 are the bands associated the transitions the Eu^{3+} ($^7F_0 \rightarrow {}^5L_J$) to the higher energy levels: $^7F_0 \rightarrow {}^5L_6$ (~394 nm), $^7F_1 \rightarrow {}^5L_7$ (~400 nm), $^7F_0 \rightarrow {}^5D_2$ (~463 nm) $^5D_1 \rightarrow {}^7F_0$ (~525 nm) $^5D_1 \rightarrow {}^7F_1$ (~532 nm). Note that the in 394 nm the transition exhibits a higher intensity compared to the band localized in 463 nm transition. Therefore, the transition $^5L_6 \rightarrow {}^7F_0$ (~394 nm) was chosen for excitation of the samples with Eu^{3+} [30–31]. Therefore, the Eu^{3+}-doped Al_2O_{3i} with 1, 2, 3 and 5 mol%, heat-treated at 400, 500, 600, 700, 800, 900 and 1000 °C, were submitted to photoluminescence emission analysis. The Fig. 7 shows the emission spectra.

Based on the analysis of the Fig. 7, taking into consideration the amount of Eu^{3+} in the alumina matrix and heat-treatment of the materials, the emission spectra when excited at 394 nm were observed for samples doped with 1, 2, 3 and 5 mol% of Eu^{3+} showed emission bands between 570 and 720 nm. The bands observed are attributed to intraconfigurational 4f–4f transitions of the Eu^{3+} originated from the $^5D_0 \rightarrow {}^7F_J$ levels ($J=0$, 1, 2, 3 and 4) [32]. The spectra obtained show the bands transitions $^5D_0 \rightarrow {}^7F_0$ (~578 nm) $^5D_0 \rightarrow {}^7F_1$ (587–594 nm), $^5D_0 \rightarrow {}^7F_2$ (611–620 nm), $^5D_0 \rightarrow {}^7F_3$ (648–652 nm) and $^7F_4 \rightarrow {}^5D_0$ (685–701 nm) [31–33]. The band assigned to the $^5D_0 \rightarrow {}^7F_2$, located around 612 nm of the electromagnetic spectrum, is known as a hypersensitive transition and it is forbidden by parity and becomes allowed when the chemical environment is distorted with absence of inversion center [23,34] .

It was observed that all samples showed photoluminescent emission properties. The presence of large emission bands is associated with the location of the Eu^{3+} in different site of symmetries in the Al_2O_3 matrix, and also the influence of the metastable γ-Al_2O_3 phase. Increasing the heat-treatment temperature provokes the change in the local structure of the Eu^{3+} due to changing the phase formation as can be seen in the X-ray diffractograms, shown in Fig. 1. Increasing of heat-treatment temperature promotes the transition from the γ-Al_2O_3 phase to the α-Al_2O_3 phase. Furthermore, the concentration of Eu^{3+} in the alumina matrix promotes an increase in the intensity of the band

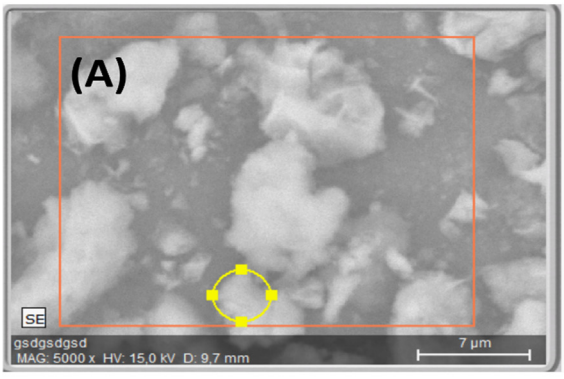

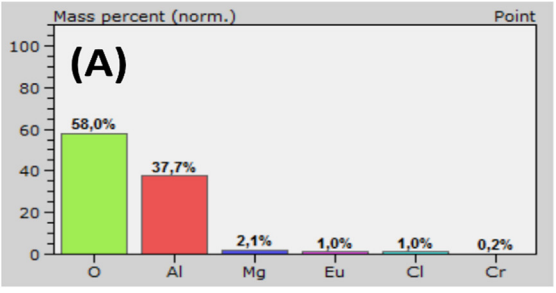

	AN	Series	nor. C [wt.%]	Atom C [at.%]	Error [%]
Oxygen	8	K series	58,00	70,44	0,00
Aluminium	13	K series	37,73	27,17	0,00
Magnesium	12	K series	2,06	1,65	0,00
Europium	63	L series	1,01	0,13	0,00
Chlorine	17	K series	0,99	0,54	0,00
Chromium	24	K series	0,21	0,08	0,00
		Total	**100,00**	**100,00**	

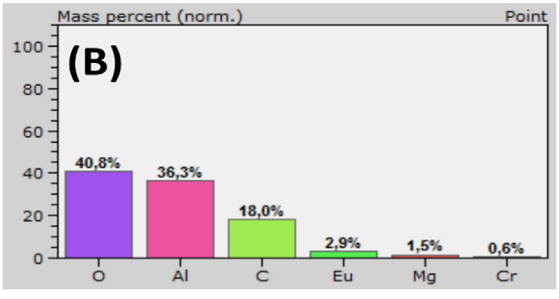

	AN	Series	nor. C [wt.%]	Atom C [at.%]	Error [%]
Oxygen	8	K series	40,79	46,51	0,00
Aluminium	13	K series	36,34	24,57	0,00
Carbon	6	K series	17,95	27,27	0,00
Europium	63	L series	2,87	0,34	0,00
Magnesium	12	K series	1,46	1,09	0,00
Chromium	24	K series	0,59	0,21	0,00
		Total	**100,00**	**100,00**	

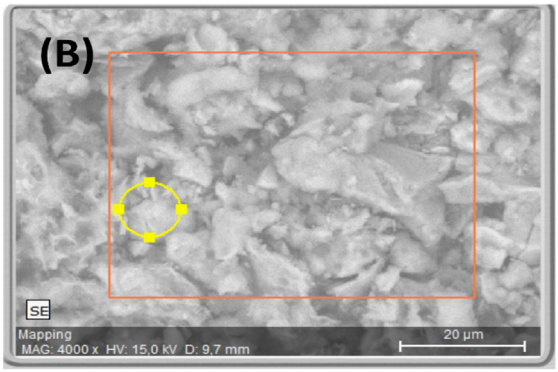

Fig. 4. EDX of the Eu^{3+}-doped Al_2O_3 samples with: (A) 1, and (B) 3 mol% of Eu^{3+} heat-treated at 400 and 700 °C respectively, for 4 h prepared by co-precipitation method .

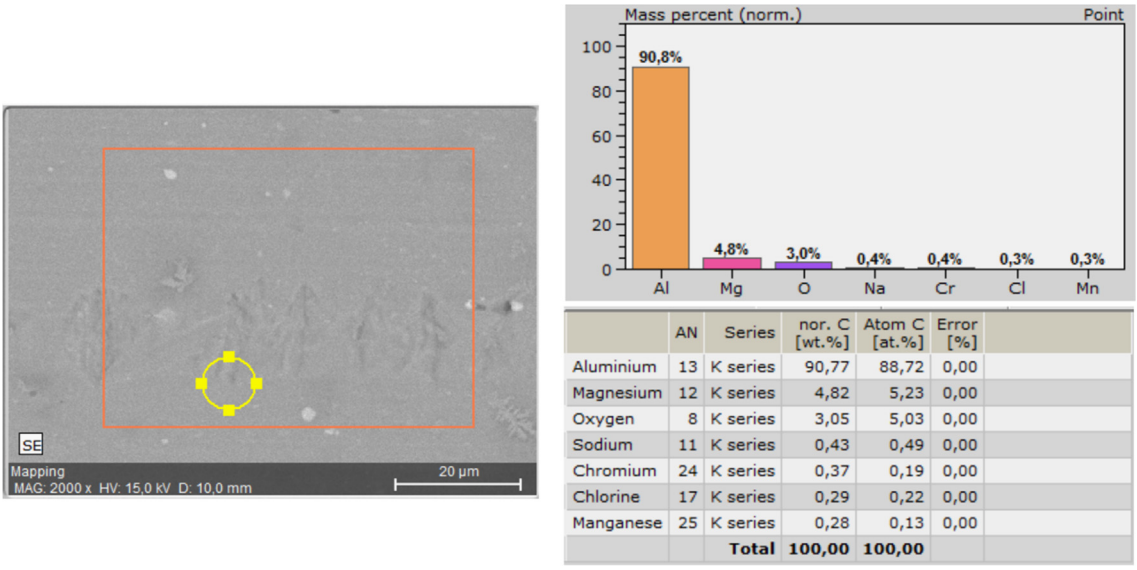

	AN	Series	nor. C [wt.%]	Atom C [at.%]	Error [%]
Aluminium	13	K series	90,77	88,72	0,00
Magnesium	12	K series	4,82	5,23	0,00
Oxygen	8	K series	3,05	5,03	0,00
Sodium	11	K series	0,43	0,49	0,00
Chromium	24	K series	0,37	0,19	0,00
Chlorine	17	K series	0,29	0,22	0,00
Manganese	25	K series	0,28	0,13	0,00
		Total	**100,00**	**100,00**	

Fig. 5. EDX analysis of the ring of aluminum cans used as a precursor for the synthesis of the materials.

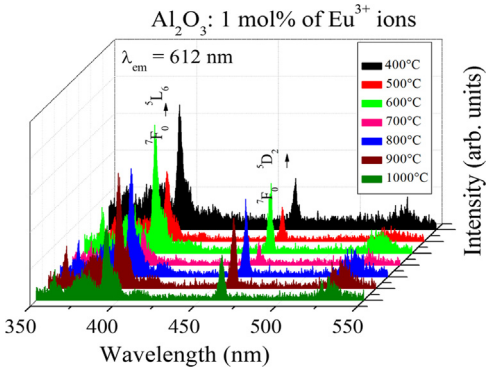

Fig. 6. Excitation spectra of the Eu^{3+}-doped Al_2O_3 samples with 1 mol% of Eu^{3+}, (λ_{em} = 612 nm), heat-treated at 500, 600, 700, 800, 900 and 1000 °C for 4 h prepared by co-precipitation method.

positioned around 693 nm assigned to the Cr^{3+}, which overlaps with the transition $^5D_0 \rightarrow {}^7F_4$ of Eu^{3+} [3]. According to the M.A.F MONTEIRO, 2008 [10], the Cr^{3+} occupies distorted octahedral sites in the crystal structure of α-Al_2O_3, with absence of symmetry with inversion center. The presence of bands around (693 nm) and (662 nm) are attributed to transitions forbidden by spin to the excited states derivatives of ^2E_g (G) and $^2T_{1g}$ (G). These doublet states are divided by spin–orbit coupling interactions, producing ruby levels (at 693 nm R_1) and (R_2 692 nm) laser used in the production [23,35]. Based on the results of the photoluminescent Eu^{3+}-doped in alumina matrix, it is suggested that the Cr^{3+} is a luminescent probe for identifying the crystalline phase α-Al_2O_3 [23,36]. The bands related the transition $^5D_0 \rightarrow {}^7F_1$, allowed by magnetic dipole, presents a radiative rate insensitive to the chemical environment, different from the transition $^5D_0 \rightarrow {}^7F_2$. Thus, the analysis of the ratio between the areas of the integrals of the transitions $^5D_0 \rightarrow {}^7F_2$ and $^5D_0 \rightarrow {}^7F_1$ allows us to assign the Eu^{3+} is located in sites of high or low symmetry. The higher the ratio of the areas, the smaller is the degree of symmetry of the crystalline region where the Eu^{3+} is surrounding. The results of the ratios of the areas are presented in Table 1.

The lifetime values of the excited state $^5D_0$ were obtained of the alumina materials doped with 1, 2, 3 and 5 mol% of Eu^{3+}. Decay curves were obtained under excitation at 394 nm and emission fixed at 612 nm ($^5D_0 \rightarrow {}^7F_2$). The decay curves showed a bi-exponential decay behavior with the correlation factor values of R=0.998. Based on the decay curves of the samples shown in Fig. 8, We calculated the average value of the lifetime by the value 1/e. The values of the lifetime of the excited state $^5D_0$ materials obtained when excited at 394 nm are shown in Table 2.

The bi-exponential decay behavior observed is consistent with the presence of more than one site of Eu^{3+} in the host matrix, confirming the enlargement of the band emission assigned to the transition of $^5D_0 \rightarrow {}^7F_J$ (J=0–4) observed in the emission spectra. The appearance of two decays were observed, with the shortest time (~0.3 m s), and another longer (~1.5 m s), which indicate the presence at least of two sites of symmetry. It was also observed that the lifetime in general for heat-treating below 600 °C, the values are relatively low in comparison to the other samples, independent of the concentration of Eu^{3+} in the matrix. The reason for this behavior can be explained by the possible existence of excited state deactivators groups, such as OH or the presence of the defects in the crystalline structure. It is possible to observe that the samples with 2 mol% of Eu^{3+} showing the longest lifetime values in comparison to other samples, independent to the heat-treatment temperature.

4. Conclusion

Based on these results, it is possible to obtain Eu^{3+}-doped Al_2O_3 photoluminescent materials with different concentrations of Eu^{3+} via a simple, rapid and cheaper synthesis using an affordable and easily accessible precursor. The materials obtained presented

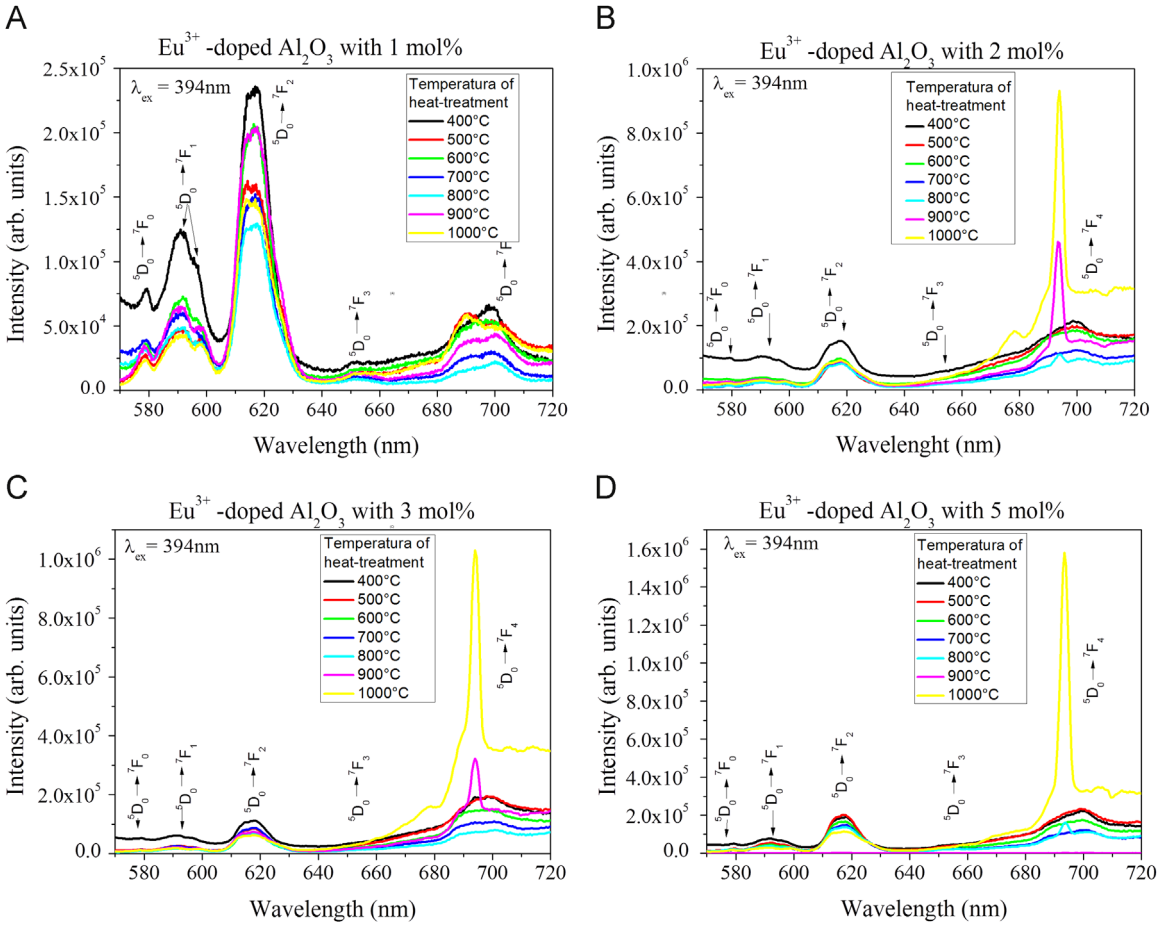

Fig. 7. Emission spectra of the Eu^{3+}-doped Al_2O_3 samples with: (A) 1, (B) 2, (C) 3, and (D) 5 mol% of Eu^{3+},(λ_{ex} = 394 nm), heat-treated at 500, 600, 700, 800, 900 and 1000 °C for 4 h prepared by co-precipitation method.

Table 1
Ratio between integrals areas of the emission bands of the samples based on Eu^{3+}-doped Al_2O_3 with : 1, 2, 3 and 5 mol%, heat-treated at 400, 500, 600, 700, 800, 900 and 1000 °C for 4 h prepared by co-precipitation method.

Ratio of the areas of the emission bands $^5D_0 \rightarrow {}^7F_2/{}^5D_0 \rightarrow {}^7F_1$				
Temperature (°C)	**% of Eu^{3+}**			
	1	**2**	**3**	**4**
400	1.74	1.28	1.67	2.25
500	3.22	2.62	2.79	3.35
600	2.66	2.22	3.26	3.53
700	2.26	3.35	3.33	3.68
800	2.46	3.26	3.54	3.42
900	3.01	2.47	3.32	1.97
1000	3.27	2.85	3.31	3.38

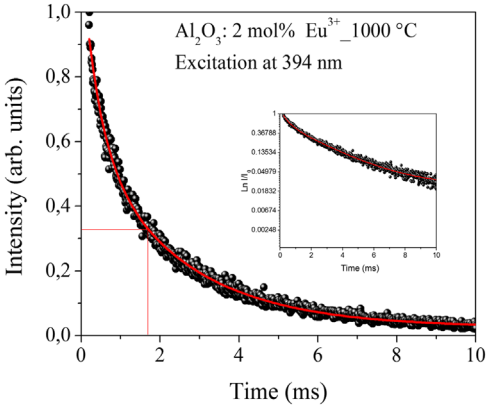

Fig. 8. Decay curve of the samples based on Eu^{3+}-doped Al_2O_3 with different percentages heated-treated at 400, 500, 600, 700, 800, 900 and 1000 °C, adjusted the an exponential decay of 2nd order, under excitation at 394 nm.

photoluminescence at different heat-treatment temperatures. Emission spectra presented broad bands indicating that the Eu^{3+} are located in different sites of symmetry due to the mixture of α and γ phases. The heat-treatment temperature played an important role in stabilizing the α-phase Al_2O_3 due to the presence of Cr^{3+} identified by the EDX analysis and the emission band localized around 693 nm. This emission is an important feature of the Cr^{3+}, which becomes a material with potential application in a far red laser region system. Furthermore, this causes the emission Cr^{3+} is used as a structural probe, indicating the formation of the crystalline phase α-Al_2O_3.

Table 2
Life time values (ms) of the samples based on the Eu^{3+}-doped Al_2O_3 with: 1, 2, 3 and 5 mol%, fixing the excitation at 394 nm and emission at 612 nm, heat-treated at 500, 600, 700, 800, 900 and 1000 °C for 4 h prepared by co-precipitation method .

Life time values (ms) of the Eu^{3+}-doped Al_2O_3 with differents percentages					
Temperature (°C)		mol% of Eu^{3+}			
		1	2	3	4
400	$1/e$	0.421	0.600	0.539	0.543
	t_1	0.253	0.271	0.217	0.257
	t_2	0.995	1.019	0.872	0.977
500	$1/e$	0.761	0.657	0.655	0.616
	t_1	0.260	0.260	0.276	0.266
	t_2	1.396	1.145	1.139	1.048
600	$1/e$	0.569	0.739	0.673	0.684
	t_1	0.275	0.275	0.270	0.273
	t_2	1.275	1.279	1.194	1.199
700	$1/e$	0.627	0.798	0.800	0.796
	t_1	0.263	0.312	0.335	0.318
	t_2	1.246	1.455	1.400	1.368
800	$1/e$	0.738	0.943	0.905	0.825
	t_1	0.341	0.321	0.367	0.294
	t_2	1.421	1.496	1.492	1.330
900	$1/e$	0.765	1.964	0.850	0.857
	t_1	0.303	0.292	0.301	0.321
	t_2	1.481	2.415	1.356	1.351
1000	$1/e$	0.822	1.500	0.775	0.823
	t_1	0.326	0.429	0.266	0.245
	t_2	1.492	2.358	1.205	1.276

Acknowledgments

The authors would like to acknowledge FAPESP, CAPES, FAPEMIG and CNPq. This work is a collaboration research project of members of the Rede Mineira de Química (RQ-MG) supported by FAPEMIG (Project: REDE-113/10). The authors acknowledge Jennifer Esbenshade for English revisions, Emílio Dias for help in the SEM analysis and also for PIIC Program Edital 001/2013/PROPE.

References

[1] N. Rakov, G.S. Maciel, Enhancement of luminescence efficiency of f–f transitions from Tb^{3+} due to energy transfer from Ce^{3+} in Al_2O_3 crystalline ceramic powders prepared by low temperature direct combustion synthesis, Chem. Phys. Lett. 400 (2004) 553–557.
[2] A. Patra, Study of photoluminescence properties of Er^{3+} ions in SiO_2–GeO_2 and Al_2O_3 nanoparticles, Solid State Commun. 132 (2004) 299–303.
[3] D. Liu, Effects of Cr content and morphology on the luminescence properties of the Cr-doped alpha-Al_2O_3 powders, Ceram. Int. 39 (2013) 4765–4769.
[4] L.E. Muresana, E.J. Popovicia, I. Perhaitaa, E. Indreab, T.D. Silipas, Effect of the europium doping on the structural and luminescent properties of yttrium aluminum garnet, Mater. Sci. Eng.: B 178 (2013) 248–253.
[5] C.H. Lu, C.H. Huang, B.M. Cheng, Synthesis and luminescence properties of microemulsion-derived $Y_3Al_5O_{12}$: Eu^{3+} phosphors, J. Alloy. Compd. 473 (2009) 376–381.
[6] S. Shikao, W. Jiye, Combustion synthesis of Eu^{3+} activated $Y_3Al_5O_{12}$ phosphor nanoparticles, J. Alloy. Compd. 327 (2001) 82–86.
[7] H. Nakajima, K. Kawano, Preparation and evaluation of the rare earth doped nanoparticle SiO_2–PVP hybrid thin film by sol–gel method, J. Alloy. Compd. 408–412 (2006) 701–705.
[8] L. Lu, X. Zhang, Z. Bai, X. Mi, Synthesis and characterization of IR up-conversion material CaS:Eu, Sm by low-temperature combustion synthesis method, Mater. Res. Bull. 44 (2009) 207–210.
[9] G. Blasse, The intensity of vibronic transitions in the spectra of the trivalent europium ion, Inorg. Chim. Acta 167 (1990) 33–37.
[10] M.A.F. Monteiro, H.F. Brito, M.C.F.C.M Felinto, G.E.S. Brito, E.E. S. Teotonio, F.M. Vichi, R. Stefani, Photoluminescence behavior of Eu^{3+} ion doped into γ- and α-alumina systems prepared by combustion, ceramic and Pechini methods, Microporous Mesoporous Mater. 108 (2008) 237–246.
[11] H.C. Jung, J.Y.G. Park, R. Seeta, R. Raju, H. Jung, B.K. Moon, J.H. Kim, H.Y. Choi, Crystalline structure dependence of luminescent properties of Eu^{3+}-activated Y_2O_3–Al_2O_3 system phosphors, Curr. Appl. Phys. 9 (2009) S217–S221.
[12] I.L.V. Rosa, A.P. Maciel, E. Longo, E.R. Leite, J.A. Varela, Synthesis and photoluminescence study of $La_{1.8}Eu_{0.2}O_3$ coating on nanometric α-Al_2O_3, Mater. Res. Bull. 41 (2006) 1791–1797.
[13] H. You, G. Hong, The change of Eu^{3+} surroundings in the system Al_2O_3–B_2O_3 containing Eu^{3+} ions, J. Phys. Chem. Solids 60 (1999) 325–329.
[14] S.M. Barros, W.M. Azevedo, H.J. Khoury, M.E.A. Andrade, P.L. Filho, Thermoluminescence study of aluminum oxide doped with therbium and thulium, Radiat. Meas. 45 (2010) 435–437.
[15] V.A. Pustovarov, V.S. Kortov, S.V. Zvonarev, A.I. Medvedev, Luminescent vacuum ultraviolet spectroscopy of Cr^{3+} ions in nanostructured aluminum oxide, J. Lumin. 132 (2012) 2868–2873.
[16] N. Rakov, G.S. Maciel, Photoluminescence analysis of α-Al_2O_3 powders doped with Eu^{3+} and Eu^{2+} ions, J. Lumin. 127 (2007) 703–706.
[17] Z. Zhu, D. Liu, H. Liu, G. Li, J. Du, Z. He, Fabrication and luminescence properties of Al_2O_3:Tb^{3+} microspheres via a microwave solvothermal route, J. Lumin. 132 (2012) 261–265.
[18] N. Rakov, W.B. Lozano, G.S. Maciel, C.B. Araújo, Nonlinear luminescence in Eu^{3+}-doped Y_2O_3 powders pumped at 355 nm, Chem. Phys. Lett. 428 (2006) 134–137.
[19] E.F. Huerta, I. Padilla, R.M. Martinez, J.L. Hernandez-Pozos, U. Caldiño, C. Falcony, Extended decay times for the photoluminescence of Eu^{3+} ions in aluminum oxide films through interaction with localized states, Opt. Mater. 34 (2012) 1137–1142.
[20] J.S. Lee, Y.J. Kim, Synthesis and luminescent properties of Al_2O_3–SiO_2 phosphors, Ceram. Int. 38 (2012) S563–S566.
[21] Z. Zhu, D. Liu, H. Liu, W. Xiaofeng, F. Lu, D. Wang, Photoluminescence properties of Tb^{3+} doped Al_2O_3 microfibers via a hydrothermal route followed by heat treatment, Ceram. Int. 38 (2012) 4137–4141.
[22] J.L. Ferrari, R.L.T. Parreira, A.M. Pires, S.A.M. Lima, A route to obtain Gd_2O_3:Nd^{3+} with different particle size, Mater. Chem. Phys. 127 (2011) 40–44.
[23] H. Liu, G. Ning, Z. Gan, Y. Lin, A simple procedure to prepare spherical α-alumina powders, Mater. Res. Bull. 44 (2009) 785–788.
[24] C. Feldmann, T. Justel, C.R. Ronda, P.J. Schmidt, Inorganic luminescent materials: 100 years of research and application, Adv. Funct. Mater. 13 (2003) 511–516.
[26] L. Trinkler, B. Berzina, Z. Jevsjutina, J. Grabis, I. Steins, C.J. Baily, Photoluminescence of Al_2O_3 nanopowders of different phases, Opt. Mater. 34 (2012) 1553–1557.
[27] P.G. Li, M. Lei, W.H. Tang, Raman and photoluminescence properties of α-Al_2O_3 microcones with hierarchical and repetitive superstructure, Mater. Lett. 64 (2010) 161–163.
[28] S. Cava, S.M. Tebcherani, S.A. Pianaro, C.A. Paskocimas, E. Longoc, J.A. Varela, Structural and spectroscopic analysis of γ-Al_2O_3 to α-Al_2O_3–$CoAl_2O_4$ phase transition, Mater. Chem. Phys. 97 (2006) 102–108.
[29] M.H. Lee, W.S. Jung, Luminescence spectra of Eu (III/II)-doped $LaAlO_3$ powders prepared by a solid-state reaction of Eu (III)-doped $LaCO_3OH$ and Al_2O_3, Ceram. Int. 40 (2014) 13419–13425.

[30] H.L. Wen, Y.Y. Chen, F.S. Yen, C.Y. Huang, Size characterization of θ- and α-Al_2O_3 crystallites during phase transformation, Nanostruct. Mater. 11 (1999) 89–101.

[31] U. Caldino, E. Álvarez, A. Speghini, M. Bettinelli, New greenish-yellow and yellowish-green emitting glass phosphors: Tb^{3+}/Eu^{3+} and $Ce^{3+}/Tb^{3+}/Eu^{3+}$ in zinc phosphate glasses, J. Lumin. 135 (2013) 216–220.

[32] O.L. Malta, S.J.L. Ribeiro, M. Faucher, P. Porcher, Theoretical intensities of 4f–4f transitions between stark levels of the Eu^{3+} ion in crystal, J. Phys. Chem. of Solids 52 (1991) 587–593.

[33] V.G. Pol, J.M. Calderon-Moreno, Fabrication of luminescent Eu_2O_3 superstructures, Chem. Phys. Lett. 1 (2010) 319–322.

[34] W. Jia, H. Liu, S.P. Felofilov, R. Melyzer, J. Jiao, Spectroscopy study of Eu^{3+}-doped and Eu^{3+}, Y^{3+}-codoped SiO_2 sol–gel glasses, J. Alloy. Compd. 311 (2000) 11–15.

[35] M.G. Brik, N.M. Avram, C.N. Avram, Crystal field analysis of energy level structure of the Cr_2O_3 antiferromagnet, Solid State Commun. 132 (2004) 831–835.

[36] V.A. Pustovarov, V.S. Kortov, Time-resolved luminescence of defect sand Cr^{3+} impurity centers in nanosized alumina crystals under vacuum-ultraviolet excitation, Tech. Phys. Lett. 38 (2012) 511–515.